Hydrogen Bonding Alteration of Thr-204 in the Complex between *pharaonis* Phoborhodopsin and Its Transducer Protein†

Yuki Sudo,‡ Yuji Furutani,§,||,⊥ Kazumi Shimono,‡ Naoki Kamo,‡ and Hideki Kandori*,§,⊥

Laboratory of Biophysical Chemistry, Graduate School of Pharmaceutical Sciences, Hokkaido University, Sapporo 060-0812, Japan, Department of Applied Chemistry, Nagoya Institute of Technology, Showa-ku, Nagoya 466-8555, Japan, Department of Biophysics, Graduate School of Science, Kyoto University, Sakyo-ku, Kyoto 606-8502, Japan, and Core Research for Evolutional Science and Technology (CREST), Japan Science and Technology Corporation, Kyoto 606-8502, Japan

Received September 16, 2003; Revised Manuscript Received October 7, 2003

ABSTRACT: *pharaonis* phoborhodopsin (*p*pR, also called *pharaonis* sensory rhodopsin II, *p*sRII) is a receptor for negative phototaxis in *Natronobacterium pharaonis*. It forms a 2:2 complex with its transducer protein, *p*HtrII, in membranes and transmits light signals through the change in the protein−protein interaction. We previously found that the *p*pR$_K$ minus *p*pR spectrum in D_2O possesses vibrational bands of *p*pR at 3479 (−)/3369 (+) cm^{-1} only in the presence of *p*HtrII [Furutani, Y., Sudo, Y., Kamo, N., and Kandori, H. (2003) *Biochemistry 42,* 4837−4842]. A D/H-unexchangeable X−H group appears to form a stronger hydrogen bond upon retinal photoisomerization in the *p*pR−*p*HtrII complex. This article aims to identify the group by use of various mutant proteins. According to the crystal structure, Tyr-199 of *p*pR forms a hydrogen bond with Asn-74 of *p*HtrII in the complex. Nevertheless, the 3479 (−)/3369 (+) cm^{-1} bands were preserved in the Y199F mutant, excluding the possibility that the bands are O−H stretches of Tyr-199. On the other hand, Thr-204 and Tyr-174 form a hydrogen bond between the retinal chromophore pocket and the binding surface of the *p*pR−*p*HtrII complex. These FTIR measurements revealed that the bands at 3479 (−)/3369 (+) cm^{-1} disappeared in the T204A mutant, while being shifted to 3498 (−) and 3474 (+) cm^{-1} in the T204S mutant. They appear at 3430 (−)/3402 (+) cm^{-1} in the Y174F mutant. From these results, we concluded that the bands at 3479 (−)/3369 (+) cm^{-1} originate from the O−H stretch of Thr-204. A stronger hydrogen bond as shown by a large spectral downshift (110 cm^{-1}) suggests that the specific hydrogen bonding alteration of Thr-204 takes place upon retinal photoisomerization, which does not occur in the absence of the transducer protein. Thr-204 has been known as an important residue for color tuning and photocycle kinetics in *p*pR. The results presented here point to an additional important role of Thr-204 in *p*pR for the interaction with *p*HtrII. Specific interaction in the complex that involves Thr-204 presumably affects the decay kinetics and binding affinity in the M intermediate.

pharaonis phoborhodopsin (*p*pR,[1] also called *pharaonis* sensory rhodopsin II, *p*sRII) is one of the archaeal rhodopsins that have *all-trans*-retinal as a chromophore (*1*−*5*). The retinal forms a Schiff base linkage with Lys-205 in the middle of the seventh transmembrane helix (*6*, *7*). *p*pR serves as a photoreceptor in *Natronobacterium pharaonis*, and forms a signaling complex in archaeal membranes with the *pharaonis* halobacterial transducer protein, *p*HtrII (*8*).

*p*HtrII is a transmembrane two-helix protein and belongs to a family of transmembrane two-helix methyl-accepting chemotaxis proteins (MCPs) (*9*, *10*). It is well-known that MCPs exist as homodimers composed of 50−60 kDa subunits and form a ternary complex with CheA and CheW. Chemical stimuli activate phosphorylation cascades that modulate flagella motors (*11*−*13*), where MCPs act not only as signal receptors but also as transducers. In contrast, light signal is received by *p*pR, a protein different from *p*HtrII. Therefore, specific interaction is required between *p*pR and *p*HtrII (*8*, *14*). *p*pR transmits light signals to *p*HtrII through the change in such an interaction, and *p*HtrII eventually activates phosphorylation cascades that modulate flagella motors. By using the signaling system, the archea avoid harmful near-UV light, displaying what is called a negative phototaxis. *p*pR absorbs maximally at 498 nm, and the light triggers *trans*−*cis* photoisomerization of the retinal chromophore in its electronically excited state (*15*), followed by rapid formation of the ground-state species such as the K intermediate. Relaxation of the K intermediate leads to functional processes during the photocycle, where protein structural changes are transmitted from *p*pR to *p*HtrII presumably in the M and/or O states (*16*).

*p*pR is stable in membranes and DM micelles (*17*, *18*), and expression in *Escherichia coli* cells can provide large

† This work was supported by grants from Japanese Ministry of Education, Culture, Sports, Science, and Technology.

* To whom correspondence should be addressed. Phone and Fax: 81-52-735-5207. E-mail: kandori@ach.nitech.ac.jp.

‡ Hokkaido University.

§ Nagoya Institute of Technology.

|| Kyoto University.

⊥ Japan Science and Technology Corp.

[1] Abbreviations: *p*pR, *pharaonis* phoborhodopsin; *p*HtrII, truncated *pharaonis* halobacterial transducer II expressed from position 1 to 159; *p*pR$_K$, K intermediate of *p*pR; DM, *n*-dodecyl β-D-maltoside; Y174F, Y199F, T204S, and T204A, *p*pR mutants in which Tyr-174, Tyr-199, and Thr-204 are substituted with Phe, Phe, Ser, and Ala, respectively; *p*pR$_M$, M intermediate of *p*pR; *p*pR$_O$, O intermediate of *p*pR; FTIR, Fourier transform infrared; PC, L-α-phosphatidylcholine.

10.1021/bi035678g CCC: $25.00
Published on Web 11/13/2003

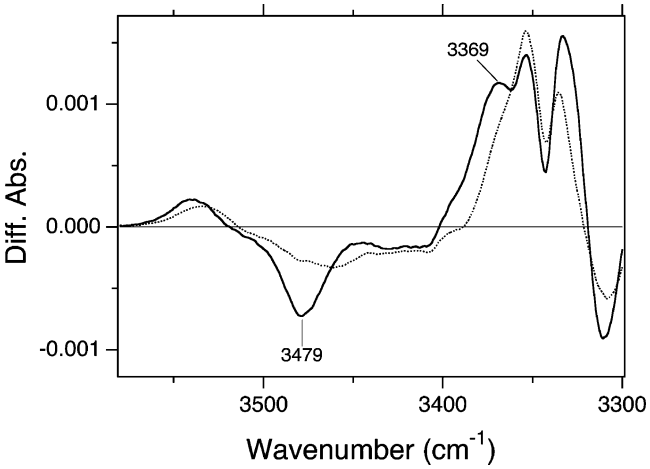

FIGURE 1: *p*pR$_K$ minus *p*pR infrared difference spectra in the absence (···) and presence (−) of *p*HtrII in the 3580−3300 cm^{-1} region. Published spectra are reproduced from ref *40*.

amounts of this protein (several milligrams per liter of culture) (*19*). Therefore, *p*pR has been well characterized over the past few years using various methods, e.g., X-ray crystallography (*6*−*8*, *20*), electron paramagnetic resonance (EPR) (*21*, *22*), electrochemistry (*23*, *24*), vibrational spectroscopy (*25*−*29*), mutagenesis (*30*, *31*), solid-state NMR (*32*), etc. On the other hand, characterization of *p*HtrII is less advanced, although ESR (*22*) and X-ray crystallographic analysis (*8*) have shown that the binding surface of *p*pR with *p*HtrII consists of helices F and G.

We and Wegener *et al*. succeeded in expressing *p*HtrII in *E. coli* (*21*, *33*), and this *p*HtrII protein has the ability to bind with *p*pR (*22*, *33*). Thus, *p*pR−*p*HtrII (complex between *p*pR and *p*HtrII) is a good model system for the signal transduction mechanism. By using this system, we demonstrated 1:1 stoichiometry in the *p*pR−*p*HtrII complex and determined binding constants between *p*pR and *p*HtrII under various conditions (*33*−*35*). In addition, we showed that Tyr-199 of *p*pR is an important amino acid residue for binding to *p*HtrII (*35*). However, detailed structural studies have not been conducted.

FTIR spectroscopy is a powerful tool for investigating protein structural changes of rhodopsins in atomic detail. Earlier, we reported structural changes in *p*pR detected by means of low-temperature FTIR spectroscopy (*26*−*28*, *36*−*39*). We also recently applied FTIR spectroscopy to the *p*pR−*p*HtrII complex (*40*).[2] In general, the spectra of the *p*pR−*p*HtrII complex for the primary K intermediate were very similar to those of *p*pR without *p*HtrII, being consistent with the crystal structure of the *p*pR−*p*HtrII complex that exhibited little structural modification of *p*pR (*8*). There were some interesting differences in the spectra of the *p*pR−*p*HtrII complex though. The most characteristic spectral feature of the *p*pR−*p*HtrII complex was the appearance of D_2O-insensitive X−H stretching vibrations. Figure 1 shows the reported *p*pR$_K$ minus *p*pR difference spectra in the absence (dotted line) and presence (solid line) of *p*HtrII measured in D_2O at 77 K (*40*). As clearly seen, the negative 3479 cm^{-1} and positive 3369 cm^{-1} bands appear only in the presence

[2] Soon after our paper (*40*) had been published, Bergo *et al*. (*51*) reported time-resolved FTIR spectra of the complex. They found several spectral changes for late intermediates.

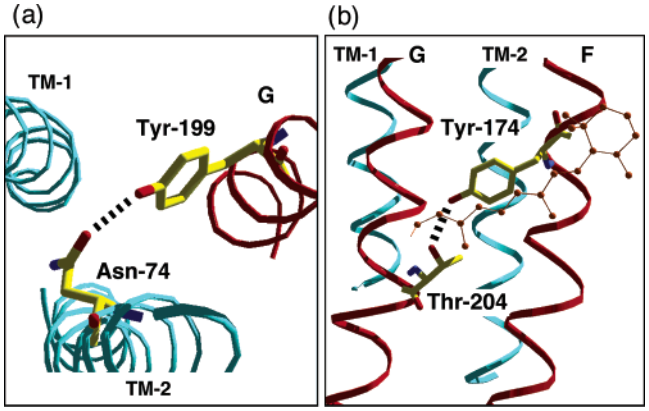

FIGURE 2: Details of the X-ray crystallographic structure of the *p*pR−*p*HtrII complex (*8*) focusing on specific hydrogen bonds. (a) Hydrogen bond between Tyr-199 of *p*pR and Asn-74 of *p*HtrII, the length of which is 2.7 Å. This view is from the cytoplasmic side along the membrane normal. (b) Hydrogen bond between Tyr-174 and Thr-204 in *p*HtrII, the length of which is 3.2 Å. This view is from the C helix side along the membrane, where helices F and G of *p*pR that involve Tyr-174 and Thr-204, respectively, are sandwiched by the retinal chromophore and helices TM-1 and TM-2 of *p*HtrII.

of *p*HtrII, providing the marker bands of the specific interaction of *p*pR and *p*HtrII. The identical spectra for the complex of the unlabeled *p*pR and ^{13}C- or ^{15}N-labeled *p*HtrII further indicate that they originate from *p*pR, not *p*HtrII (*40*).

What is the origin of the 3479 (−)/3369 (+) cm^{-1} bands? The frequency at 3479 cm^{-1} for the unphotolyzed state is considerably higher than amide A vibrations, implying that the X−H stretching vibration originates from an amino acid side chain, such as an O−H or N−H group. We have so far identified vibrational bands in this frequency region for bacteriorhodopsin and bovine rhodopsin. In the case of bacteriorhodopsin, the 3486 cm^{-1} band for the L intermediate was assigned to the D/H-unexchangeable N−H stretch of indole of Trp-182 (*41*). In bovine rhodopsin, isomer-specific bands at 3463 (11-*cis*), 3487 (*all-trans*), and 3481 cm^{-1} (9-*cis*) were assigned to the D/H-unexchangeable O−H stretch of Thr-118 (*42*). These findings provided insights into the specific protein structural changes in bacteriorhodopsin and bovine rhodopsin.

It should be noted that in the case of *p*pR, the complex with the transducer is required for the appearance of the 3479 (−)/3369 (+) cm^{-1} bands. In this regard, the first candidate may be the O−H stretch of Tyr-199, because the X-ray crystallography revealed that Tyr-199 of *p*pR forms a hydrogen bond with Asn-74 of *p*HtrII in the *p*pR−*p*HtrII complex (Figure 2a) (*8*). We have also reported that Tyr-199 is an important residue in the interaction with *p*HtrII (*35*). The O−H stretching frequency of phenol is located at 3620−3590 or 3400−3230 cm^{-1} without or with a hydrogen bond, respectively (*43*). Another candidate may be found in the interaction between Tyr-174 and Thr-204 (Figure 2b), both of which possess O−H groups and are hydrogen bonded to each other. They are located near the retinal Schiff base bound to Lys-205 and the binding surface of the *p*pR−*p*HtrII complex. Tyr-174 is completely conserved in archaeal rhodopsins (the corresponding amino acid in bacteriorhodopsin is Tyr-185) (*44*). In contrast, Thr-204 is unique for *p*pR. Bacteriorhodopsins, halorhodopsins, and sensory rhodopsins I commonly possess Ala at this position (*44*), and only

phoborhodopsins possess threonine or serine, suggesting an important role for the O−H group. Thr-204 has been known as an important residue for color tuning (*45*) and photocycle kinetics (*30*) in *p*pR.

In this study, we attempted to assign the pair of bands at 3479 (−) and 3369 (+) cm^{-1} (Figure 1) by using *p*pR mutants. Low-temperature FTIR spectroscopy of the complex suggested that the 3479 (−)/3369 (+) cm^{-1} bands do not originate from O−H stretches of Tyr-199 and Tyr-174 but originate from the O−H stretch of Thr-204. The O−H group proton cannot be exchanged in D_2O, and the hydrogen bond is greatly strengthened upon retinal photoisomerization. Since such structural change takes place only in the *p*pR−*p*HtrII complex, Thr-204 should play an important role in *p*pR for the interaction with *p*HtrII.

MATERIALS AND METHODS

Preparation of the ppR−pHtrII Complex. Expression plasmids of the wild-type, Y199F mutant, and T204A mutant proteins of *p*pR and *p*HtrII were constructed as previously described (*26*, *33*, *35*, *45*). For preparation of the Y174F and T204S gene of *p*pR, a Quickchange site-directed mutagenesis kit (Stratagene, La Jolla, CA) was used with the template for polymerase chain reaction pFE/*p*pRHis. The *p*pR and *p*HtrII proteins possessing a histidine tag at the C-terminus were expressed in *E. coli*, solubilized with 1.0% *n*-dodecyl *β*-D-maltoside (DM), and purified with a Ni column as described previously (*26*). The chromophore configuration of the mutant *p*pR was examined by using an HPLC column chromatography as described previously (*46*), which showed that all mutants (Y199F, Y174F, T204A, and T204S) have *all-trans*-retinal only, similar to wild-type *p*pR. The purified *p*pR and *p*HtrII proteins were mixed in a 1:1 molar ratio, and incubated for 1 h at 4 °C.

Complex formation in the mutant proteins was confirmed by comparing the decay kinetics of $p$ppR$_M$ in the presence and absence of *p*HtrII, taking into account the fact that the decay of M is ca. 2-fold slower in the *p*pR−*p*HtrII complex (*33*). If the complex is formed in mutants, this measurement also provides binding parameters (K_D, dissociation constant, and n, the number of binding sites) in the M state as described for wild-type *p*pR (*33*). In the study presented here, the *p*HtrII concentration was kept constant (25 μM), and the rates of M decay were measured by flash spectroscopy under the varying concentrations of the *p*pR mutant. From the titration curves, K_D and n values were determined.

FTIR Spectroscopy. Low-temperature FTIR spectroscopy was performed as described previously (*26*, *27*). For the IR measurements, the *p*pR−*p*HtrII mixture was reconstituted into L-α-phosphatidylcholine (PC) liposomes (*p*pR:PC molar ratio of 1:50), where DM was removed by dialysis. The *p*pR−*p*HtrII complexes in the PC liposomes were washed three times with a buffer at pH 7.0 (2 mM phosphate). Then 90 μL of the *p*pR−*p*HtrII complex sample was dried on a BaF_2 window with a diameter of 18 mm. After hydration by D_2O, the sample was placed in a cell, which was mounted in an Oxford DN-1704 cryostat placed in the Bio-Rad FTS-40 spectrometer. Illumination with 450 nm light at 77 K for 2 min converted *p*pR to $p$ppR$_K$, and subsequent illumination with >560 nm light forced $p$ppR$_K$ to revert to *p*pR as described previously (*26*, *40*). The difference spectrum was calculated from the spectra constructed from 128 interferograms before and after the illumination. Twenty-four spectra obtained in this way were averaged to obtain the $p$ppR$_K$ minus *p*pR spectra except for that for Y174F. In the case of Y174F, the spectrum by photoreversion of $p$ppR$_K$ to *p*pR was not a mirror image of the $p$ppR$_K$ minus *p*pR spectrum (forward photoreaction). Therefore, three spectra obtained by illumination with 450 nm light were averaged to obtain the $p$ppR$_K$ minus *p*pR spectrum of Y174F.

RESULTS

Formation of the Complex between the Mutant ppR and pHtrII. Before using FTIR spectroscopy, we examined various properties of the mutant proteins. First, HPLC column chromatography showed that all the mutants (Y199F, Y174F, T204A, and T204S) have *all-trans*-retinal only, similar to wild-type *p*pR. This fact suggests that these mutations do not cause structural changes in the retinal binding pocket. Y199F has a visible absorption spectrum identical to that of the wild type (λ_{max} = 498 nm). In contrast, the other mutants possess red-shifted visible absorption spectra, the λ_{max} values of which were 502, 504, and 509 nm for Y174F, T204S, and T204A, respectively. This fact suggests that the hydrogen bonding interaction between Tyr-174 and Thr-204 is involved in the blue spectral shift in *p*pR.

M decay kinetics were then compared in the absence and presence of *p*HtrII for all mutants. We found that the M decay kinetics of all mutants were delayed in the presence of *p*HtrII (data not shown), confirming the complex formation in these mutant proteins. In addition, kinetic measurements with different *p*pR concentrations allowed determinations of the dissociation constants and the stoichiometry of the complex between $p$ppR$_M$ and *p*HtrII. For all mutants, the stoichiometry was 1:1. While the K_D value of Y199F (14.0 μM) was close to that of the wild type (15.2 μM), the K_D values of T204A and T204S were estimated to be 3.8 and 4.8 μM, respectively, implying a stronger binding of $p$ppR$_M$ with *p*HtrII in the T204 mutants. In the wild type, the K_D of the unphotolyzed state is 0.15 μM, which increases ∼100 times in the M state (*33*, *34*). This indicates that signal transduction from *p*pR to *p*HtrII involves weakening of their interaction in M. Less pronounced weakening of the interaction in M for the T204 mutants suggests the important role of Thr-204 in the signal transduction. In case of Y174F, the M decay could not be fitted by a single exponential, which made it difficult to determine the accurate K_D value. It should be noted, however, that the M decay was delayed in Y174F in a manner analogous to that of the other mutants.

FTIR Spectrum of the Complex between the Y199F Mutant ppR and pHtrII. Figure 3 shows the $p$ppR$_K$ minus *p*pR infrared difference spectra of Y199F (solid line) and the wild type (dotted line) in the presence of *p*HtrII. Both spectra coincide well in the 3580−3300 cm^{-1} region, and the spectrum of Y199F possesses the bands at 3479 (−)/3369 (+) cm^{-1}. Therefore, these bands do not originate from an O−H stretching vibration of Tyr-199. In addition, both spectra coincide well in other frequency regions, indicating that the mutation of Tyr-199 does not affect protein structural changes upon formation of the K intermediate in the *p*pR−*p*HtrII complex.

FTIR Spectrum of the Complex between the Y174F ppR Mutant and pHtrII. Figure 4 shows the $p$ppR$_K$ minus *p*pR

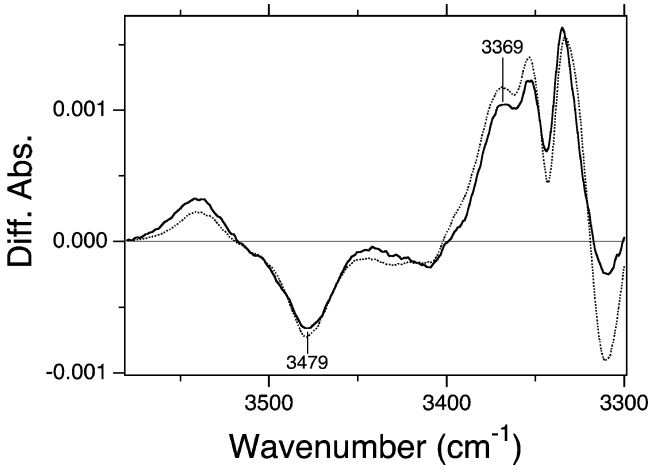

FIGURE 3: *p*pR$_K$ minus *p*pR infrared difference spectra of Y199F (−) and the wild type (···) of *p*pR in the presence of *p*HtrII in the 3580−3300 cm^{-1} region. Spectra were recorded at 77 K and pH 7 upon hydration with D_2O.

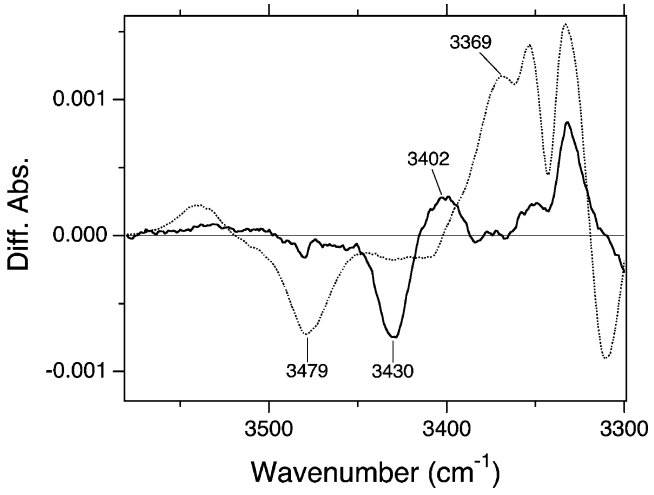

FIGURE 4: *p*pR$_K$ minus *p*pR infrared difference spectra of Y174F (−) and the wild type (···) of *p*pR in the presence of *p*HtrII in the 3580−3300 cm^{-1} region. Spectra were recorded at 77 K and pH 7 upon hydration with D_2O.

infrared difference spectra of Y174F (solid line) and the wild type (dotted line) in the presence of *p*HtrII. In contrast to those of Y199F, the spectra look very different for Y174F. Such spectral differences caused by the mutation were observed in the entire mid-infrared region, although the 1204 (−)/1194 (+) cm^{-1} bands clearly demonstrated normal photoisomerization from *all-trans*- to 13-*cis*-retinal in Y174F (data not shown). Tyr-174 forms a hydrogen bond not only with Thr-204 but also with Asp-201, one of the participants in the counterion complex of *p*pR. Cleavage of the important hydrogen bond between Tyr-174 and Asp-201 may significantly affect the FTIR spectra. A similar observation was reported for the corresponding Y185F mutant of bacteriorhodopsin (*47*).

It should be noted that the negative band at 3430 cm^{-1} in Y174F looks similar to that at 3479 cm^{-1}. Our previous reports on bacteriorhodopsin and bovine rhodopsin showed that there is a limited number of vibrational bands that appear in the >3400 cm^{-1} region in D_2O for the photoreactions at 77 K (*42*, *48*). Therefore, it is possible that the negative 3479 cm^{-1} band in the wild type is shifted to 3430 cm^{-1} in Y174F. If it is, the corresponding positive band may be at 3402 cm^{-1},

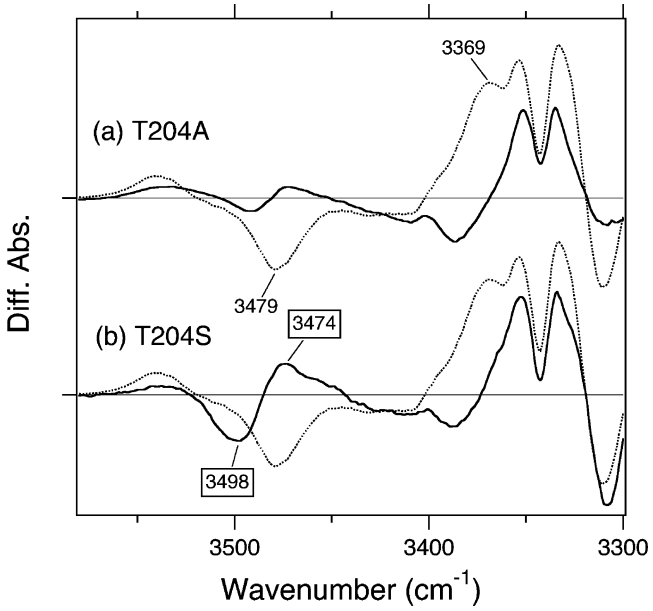

FIGURE 5: *p*pR$_K$ minus *p*pR infrared difference spectra of T204A (solid line in part a), T204S (solid line in part b), and the wild type (dotted lines) of *p*pR in the presence of *p*HtrII in the 3580−3300 cm^{-1} region. Spectra were recorded at 77 K and pH 7 upon hydration with D_2O.

suggesting that the bands at 3479 (−)/3369 (+) cm^{-1} do not originate from the O−H stretching vibration of Tyr-174. Thus, multiple spectral differences of Y174F made it difficult to conclude if the bands originate from the O−H stretch of Tyr-174, whereas the mutation of Tyr-174 clearly influences the bands.

FTIR Spectra of the Complex between the T204A or T204S ppR Mutant and pHtrII. Solid lines in Figure 5 represent the *p*pR$_K$ minus *p*pR infrared difference spectra of T204A (a) and T204S (b), being shown with that of the wild type (dotted line). In these mutants, there are some spectral differences from the wild type in other frequency regions. For instance, the ethylenic C═C stretches at 1553 (−)/1544 (+) cm^{-1} of the wild type are shifted to 1549 (−)/1536 (+) and 1550 (−)/1537 (+) cm^{-1} in T204A and T204S, respectively, being consistent with the spectral red shifts in these mutants (data not shown). However, spectral differences were much smaller in the Thr-204 mutants than in Y174F.

Figure 5a shows that both 3479 (−) and 3369 (+) cm^{-1} bands disappear in T204A. Disappearance of the 3479 (−) and 3369 (+) cm^{-1} bands was also observed in T204S, whereas new bands appeared at 3498 (−) and 3474 (+) cm^{-1} (Figure 5b). These observations strongly suggest that the bands at 3479 (−) and 3369 (+) cm^{-1} originate from the O−H stretch of Thr-204. The O−H stretch of Ser-204 in T204S should be at 3498 and 3474 cm^{-1} for *p*pR and *p*pR$_K$, respectively.

Secondary alcohols possess their O−H stretches at 3626−3629 and 3340−3355 cm^{-1} in CCl_4 solution and in neat liquid, respectively (*43*). The O−H stretching vibration of threonine, therefore, must be located anywhere from ∼3630 to 3340 cm^{-1}, depending on its hydrogen bonding conditions. The observed frequency in *p*pR at 3479 cm^{-1} corresponds to moderate hydrogen bonding. Similar O−H stretches have been reported for Thr-17 (3462 cm^{-1}) in bacteriorhodopsin (*48*) and Thr-118 (3463 cm^{-1}) in bovine rhodopsin (*42*). The

retinal photoisomerization induces a frequency downshift of the O−H stretch of Thr-204 by 110 cm^{-1} in *p*pR. The observed frequency in *p*pR_K at 3369 cm^{-1} is close to the value in neat liquid, indicating that the hydrogen bond is very strong (*43*). Similar O−H stretches have been reported for Thr-89 in bacteriorhodopsin and Thr-79 in *p*pR, which are D/H-exchangeable and appear at ~2510 cm^{-1} as O−D stretches (*49*, *50*).

DISCUSSION

In this paper, we attempted to assign the D_2O-insensitive X−H vibrational bands of *p*pR at 3479 (−)/3369 (+) cm^{-1}, which appear in the *p*pR_K minus *p*pR infrared difference spectra only for the *p*pR−*p*HtrII complex (Figure 1). Using the X-ray crystallographic structure (*8*), we first examined the possibility that the bands originate from the O−H stretches of Tyr-199 (Figure 2a). However, the bands were preserved in Y199F (Figure 3), so the bands do not originate from the O−H stretch of Tyr-199. The *p*pR_K minus *p*pR difference spectra were identical for Y199F and the wild type, indicating that the mutation from Tyr to Phe at position 199 does not affect protein structural changes upon formation of the K intermediate in the *p*pR−*p*HtrII complex. Since the side chain of Tyr-199 is located more than 10 Å from the retinal chromophore, no spectral changes for the *p*pR_K minus *p*pR spectra could be expected.

Then, we focused on a hydrogen bond inside *p*pR. The distance between the side chain oxygens of Tyr-174 and Thr-204 is 3.2 Å (Figure 6), and it is sandwiched by the retinal chromophore and the binding surface of the *p*pR−*p*HtrII complex (Figure 2b). The bands at 3479 (−)/3369 (+) cm^{-1} disappeared in T204A, while being upshifted to 3498 (−)/3474 (+) cm^{-1} in T204S (Figure 4). Although we have not used isotope labeling of threonine, the mutant analysis presented here strongly suggests that the bands at 3498 (−) and 3474 (+) cm^{-1} originate from the O−H stretch of Thr-204.

The O−H stretch of Thr-204 in the *p*pR−*p*HtrII complex at 3479 cm^{-1} corresponds to moderate hydrogen bonding. According to the X-ray crystal structure of the *p*pR−*p*HtrII complex (*8*), the hydrogen bonding distance from the side chain oxygen of Thr-204 to the peptide carbonyl oxygen of Leu-200 and the phenolic oxygen of Tyr-174 is 2.8 and 3.2 Å, respectively (Figure 6). The presence of such hydrogen bonding acceptors is consistent with the present IR observation. Upon retinal photoisomerization, the frequency of the O−H stretch of Thr-204 is lowered by 110 cm^{-1} in the *p*pR_K−*p*HtrII complex, whereas no such bands were observed in the absence of *p*HtrII (Figure 1). Why does the O−H group of Thr-204 change its hydrogen bonding only in the presence of *p*HtrII? Why does it not in the absence of *p*HtrII? Interestingly, the hydrogen bonding network around Thr-204 is essentially similar in the free *p*pR (*6*, *7*) and *p*pR−*p*HtrII complex (*8*) (Figure 6), suggesting that structural changes are different between them. The latter question may be examined by structural comparison of transducer-free *p*pR (*6*, *7*) and *p*pR_K (*20*). There are no changes in distances between Thr-204 and Tyr-174 (3.3 Å in *p*pR and 3.4 Å in *p*pR_K) and between Thr-204 and Leu-200 (2.9 Å in *p*pR and *p*pR_K) (*6*, *7*, *20*), being consistent with absence of the spectral shift of the O−H stretch of Thr-204 in the transducer-free *p*pR.

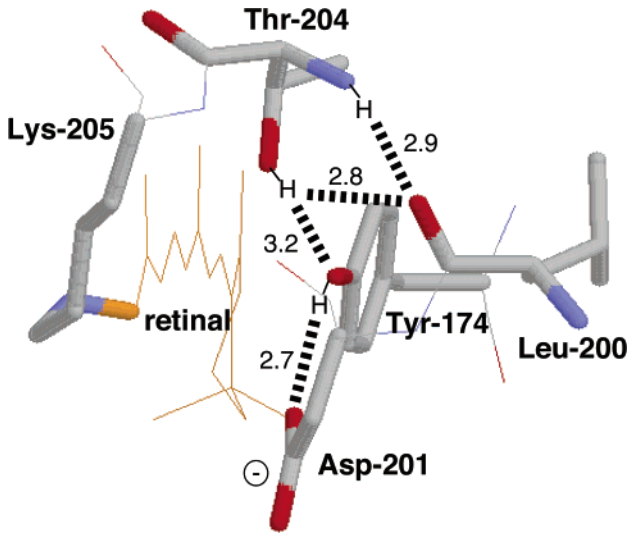

FIGURE 6: X-ray crystallographic structure of the region of Thr-204 and Tyr-174 in the *p*pR−*p*HtrII complex (*8*). The membrane normal is roughly in the vertical plane of this figure. Top and bottom regions correspond to the cytoplasmic and extracellular sides, respectively. Retinal chromophore and peptide backbones except for Leu-200 and Thr-204 are shown with wireframe drawings. Hydrogen atoms and hydrogen bonds are inferred from the structure, where the numbers give the hydrogen bonding distances in angstroms. It should be noted that the transducer-free *p*pR (*6*, *7*) shows essentially similar structure in this region, though the distance between Thr-204 and Tyr-174 is slightly longer (3.5 Å). The greatest difference between the transducer-free *p*pR (*6*, *7*) and the *p*pR−*p*HtrII complex (*8*) in this region is the retinal conformation. In the *p*pR−*p*HtrII complex, the C14−C15 single bond possesses a *cis* conformation (more clearly shown in Figure 2b), which is entirely different from the relaxed *all-trans* chromophore in the unphotolyzed state of archaeal rhodopsins. As a consequence, the Schiff base N−H group points toward the cytoplasmic side, being in the opposite direction in the transducer-free *p*pR. However, no spectroscopic evidence has been provided in support of the C14−C15 *cis* conformation.

Unlike in the free *p*pR, the O−H group of Thr-204 exhibits a frequency downshift of 110 cm^{-1} upon retinal photoisomerization in the *p*pR−*p*HtrII complex. The O−H stretch in *p*pR_K at 3369 cm^{-1} corresponds to very strong hydrogen bonding, because the value is close to those in neat liquid of secondary alcohols (*43*). What is the hydrogen bonding acceptor in *p*pR_K? Although the X-ray crystal structure of the *p*pR_K−*p*HtrII complex has not been reported, the FTIR study of mutants presented here may provide suggestions. If threonine is replaced with serine at position 204, the spectral downshift is only 24 cm^{-1} (Figure 5b), and the O−H stretch at 3474 cm^{-1} in *p*pR_K is not strong. This fact suggests that the hydrogen bonding alteration of the O−H group is highly sensitive to its environment. If Tyr-174 is replaced with Phe, the O−H stretch of Thr-204 seems to appear at 3430 (−) and 3402 (+) cm^{-1} (Figure 4). While the O−H stretch at 3430 cm^{-1} in Y174F indicates a strong hydrogen bond for Thr-204, a small spectral downshift of 28 cm^{-1} upon retinal isomerization in Y174F also implies that the hydrogen bonding alteration of the O−H group is highly sensitive to its environment.

Strong hydrogen bonds of threonine have been so far reported for Thr-89 in bacteriorhodopsin and Thr-79 in *p*pR, which are D/H-exchangeable and appear at ~2510 cm^{-1} as the O−D stretches (*49*, *50*). In case of Thr-89 in bacteriorhodopsin, the corresponding O−H stretches were estimated

to be 3378 and 3317 cm^{-1} for the unphotolyzed state and the K intermediate, respectively (*49*). In these cases, strong hydrogen bonds of threonine side chains are reasonable, because their hydrogen bonding acceptors are negatively charged aspartates (Asp-85 in bacteriorhodopsin and Asp-75 in *p*pR). In the *p*pR_K−*p*HtrII complex, the hydrogen bonding acceptor of the O−H group of Thr-204 could be (i) the peptide carbonyl of Leu-200, (ii) the phenolic oxygen of Tyr174, or (iii) the side chain oxygen of Asp-201 (Figure 6). Among them, only Asp-201 possesses a negative charge, whereas the distance between the side chain oxygens of Thr-204 and Asp201 is 4.6 Å in the *p*pR−*p*HtrII complex. Since the protein structural changes are limited for the formation of K at 77 K, a significantly shortened distance between Thr-204 and Asp-201 would be unlikely. If the hydrogen bonding acceptor is Tyr-174, such a frequency downshift may be the consequence of the partial negative charge on the phenolic oxygen of Tyr-174 in *p*pR_K.

We have studied hydrogen bonding alterations of threonine side chains in bacteriorhodopsin, and bovine rhodopsin. It is particularly important to note that at 77 K the frequency changes are not large in general, since protein structural changes are very limited. We have reported that the frequency shifts at 77 K are 18 cm^{-1} for Thr-17, 13 cm^{-1} for Thr-121, and ~60 cm^{-1} for Thr-89 in bacteriorhodopsin (*48*, *49*), and 24 cm^{-1} for Thr-118 in bovine rhodopsin (*42*). Accordingly, the observation of a spectral shift of 110 cm^{-1} is unique among rhodopsins, implying a specific structural change. Complex formation with *p*HtrII allows specific hydrogen bonding alteration of Thr-204 upon formation of *p*pR_K.

Several functionally important roles of Thr-204 have been reported so far. Thr-204 is an important residue for color tuning of *p*pR, since T204A has a significantly red-shifted absorption maximum (*45*). Thr-204 should be involved in the regulation mechanism of the decay process of *p*pR_O, because the decay of *p*pR_O in T204S becomes greatly accelerated like that of bacteriorhodopsin (unpublished data). In addition, Engelhard and co-workers suggested that Thr-204 may be important for the creation of bacteriorhodopsin-like functional properties by using a quadruple mutant, which includes T204A (*30*). The study presented here has provided an additional important role for Thr-204 in the *p*pR−*p*HtrII complex. Specific interaction in the complex that involves Thr-204 presumably affects the decay kinetics and binding affinity in the M intermediate.

In conclusion, we have assigned the D_2O-insensitive O−H stretching bands at 3479 (−)/3369 (+) cm^{-1} as the O−H stretch of Thr-204 in *p*pR. A large spectral downshift of 110 cm^{-1} at 77 K is unique, indicating that hydrogen bonding interaction is greatly altered, which takes place only in the *p*pR−*p*HtrII complex. While Thr-204 has been known as an important residue for color tuning and photocycle kinetics of *p*pR, the results presented here provide an additional important role for Thr-204 in *p*pR for the interaction with *p*HtrII.

ACKNOWLEDGMENT

We thank M. Yamabi for helping in sample preparation of the Y174F mutant and Dr. M. Iwamoto for valuable discussion.

REFERENCES

1. Imamoto, Y., Shichida, Y., Hirayama, J., Tomioka, H., Kamo, N., and Yoshizawa, T. (1992) *Biochemistry 31*, 2523−2528.
2. Kamo, N., Shimono, K., Iwamoto, M., and Sudo, Y. (2001) *Biochemistry (Moscow) 66*, 1277−1282.
3. Spudich, J. L., and Luecke, H. (2002) *Curr. Opin. Struct. Biol. 12*, 540−546.
4. Spudich, J. L. (2002) *Nat. Struct. Biol. 9*, 797−799.
5. Pebay-Peyroula, E., Royant, A., Landau, E. M., and Navarro, J. (2002) *Biochim. Biophys. Acta 1565*, 196−205.
6. Luecke, H., Schobert, B., Lanyi, J. K., Spudich, E. N., and Spudich, J. L. (2001) *Science 293*, 1499−1503.
7. Royant, A., Nollert, P., Edman, K., Neutze, R., Landau, E. M., Pebay-Peyroula, E., and Navarro, J. (2001) *Proc. Natl. Acad. Sci. U.S.A. 98*, 10131−10136.
8. Gordeliy, V. I., Labahn, J., Moukhametzianov, R., Efremov, R., Granzin, J., Schlesinger, R., Büldt, G., Savopol, T., Scheidig, A. J., Klare, J. P., and Engelhard, M. (2002) *Nature 419*, 484−487.
9. Rudolph, J., Nordmann, B., Storch, K. F., Gruenberg, H., Rodewald, K., and Oesterhelt, D. (1996) *FEMS Microbiol. Lett. 139*, 161−168.
10. Falke, J. J., Bass, R. B., Butler, S. L., Chervitz, S. A., and Danielson, M. A. (1997) *Annu. Rev. Cell Dev. Biol. 13*, 457−512.
11. Alley, M. R., Maddock, J. R., and Shapiro, L. (1993) *Science 259*, 1754−1757.
12. Maddock, J. R., and Shapiro, L. (1993) *Science 259*, 1717−1723.
13. Rudolph, J., and Oesterhelt, D. (1996) *J. Mol. Biol. 258*, 548−554.
14. Zhang, X. N., Zhu, J., and Spudich, J. L. (1999) *Proc. Natl. Acad. Sci. U.S.A. 96*, 857−862.
15. Kandori, H., Tomioka, H., and Sasabe, H. (2002) *J. Phys. Chem. A 106*, 2091−2095.
16. Yan, B., Takahashi, T., Johnson, R., and Spudich, J. L. (1991) *Biochemistry 30*, 10686−10692.
17. Ikeura, Y., Shimono, K., Iwamoto, M., Sudo, Y., and Kamo, N. (2003) *Photochem. Photobiol. 77*, 96−100.
18. Sudo, Y., Yamabi, M., Iwamoto, M., Shimono, K., and Kamo, N. (2003) *Photochem. Photobiol. 78*, 503−508.
19. Shimono, K., Iwamoto, M., Sumi, M., and Kamo, N. (1997) *FEBS Lett. 420*, 54−56.
20. Edman, K., Royant, A., Nollert, P., Maxwell, C. A., Pebay-Peyroula, E., Navarro, J., Neutze, R., and Landau, E. M. (2002) *Structure 10*, 473−482.
21. Wegener, A. A., Chizhov, I., Engelhard, M., and Steinhoff, H. J. (2000) *J. Mol. Biol. 301*, 881−891.
22. Wegener, A. A., Klare, J. P., Engelhard, M., and Steinhoff, H. J. (2001) *EMBO J. 20*, 5312−5319.
23. Sudo, Y., Iwamoto, M., Shimono, K., Sumi, M., and Kamo, N. (2001) *Biophys. J. 80*, 916−922.
24. Schmies, G., Engelhard, M., Wood, P. G., Nagel, G., and Bamberg, E. (2001) *Proc. Natl. Acad. Sci. U.S.A. 98*, 1555−1559.
25. Gellini, C., Luttenberg, B., Sydor, J., Engelhard, M., and Hildebrandt, P. (2000) *FEBS Lett. 472*, 263−266.
26. Kandori, H., Shimono, K., Sudo, Y., Iwamoto, M., Shichida, Y., and Kamo, N. (2001) *Biochemistry 40*, 9238−9246.
27. Kandori, H., Furutani, Y., Shimono, K., Shichida, Y., and Kamo, N. (2001) *Biochemistry 40*, 15693−15698.
28. Kandori, H., Shimono, K., Shichida, Y., and Kamo, N. (2002) *Biochemistry 41*, 4554−4559.
29. Hein, M., Wegener, A. A., Engelhard, M., and Siebert, F. (2003) *Biophys. J. 84*, 1208−1217.
30. Klare, J. P., Schmies, G., Chizhov, I., Shimono, K., Kamo, N., and Engelhard, M. (2002) *Biophys. J. 82*, 2156−2164.
31. Shimono, K., Hayashi, T., Ikeura, Y., Sudo, Y., Iwamoto, M., and Kamo, N. (2003) *J. Biol. Chem. 278*, 23882−23889.
32. Arakawa, T., Shimono, K., Yamaguchi, S., Tuzi, S., Sudo, Y., Kamo, N., and Saito, H. (2003) *FEBS Lett. 536*, 237−240.
33. Sudo, Y., Iwamoto, M., Shimono, K., and Kamo, N. (2001) *Photochem. Photobiol. 74*, 489−494.
34. Sudo, Y., Iwamoto, M., Shimono, K., and Kamo, N. (2002) *J. Photochem. Photobiol., B 67*, 171−176.
35. Sudo, Y., Iwamoto, M., Shimono, K., and Kamo, N. (2002) *Biophys. J. 83*, 427−432.
36. Shimono, K., Furutani, Y., Kandori, H., and Kamo, N. (2002) *Biochemistry 41*, 6504−6509.
37. Furutani, Y., Iwamoto, M., Shimono, K., Kamo, N., and Kandori, H. (2002) *Biophys. J. 83*, 3482−3489.

38. Iwamoto, M., Furutani, Y., Kamo, N., and Kandori, H. (2003) *Biochemistry 42*, 2790−2796.
39. Furutani, Y., and Kandori, H. (2002) *Mol. Membr. Biol. 19*, 257−265.
40. Furutani, Y., Sudo, Y., Kamo, N., and Kandori, H. (2003) *Biochemistry 42*, 4837−4842.
41. Yamazaki, Y., Sasaki, J., Hatanaka, M., Kandori, H., Maeda, A., Needleman, R., Shinada, T., Yoshihara, K., Brown, L. S., and Lanyi, J. K. (1995) *Biochemistry 34*, 577−582.
42. Nagata, T., Oura, T., Terakita, A., Kandori, H., and Shichida, Y. (2002) *J. Phys. Chem. A 106*, 1969−1975.
43. Lin-Vien, D., Colthup, N. B., Fateley, W. G., and Grasselli, J. G. (1991) *The Handbook of Characteristic Frequencies of Organic Molecules*, Academic Press, San Diego.
44. Zhang, W., Brooun, A., Mueller, M. M., and Alam, M. (1996) *Proc. Natl. Acad. Sci. U.S.A. 93*, 8230−8235.
45. Shimono, K., Iwamoto, M., Sumi, M., and Kamo, N. (2000) *Photochem. Photobiol. 72*, 141−145.
46. Shimono, K., Ikeura, Y., Sudo, Y., Iwamoto, M., and Kamo, N. (2001) *Biochim. Biophys. Acta 1515*, 92−100.
47. Braiman, M. S., Mogi, T., Stern, L. J., Hackett, N. R., Chao, B. H., Khorana, H. G., and Rothschild, K. J. (1988) *Proteins 3*, 219−229.
48. Kandori, H., Kinoshita, N., Yamazaki, Y., Maeda, A., Shichida, Y., Needleman, R., Lanyi, J. K., Bizounok, M., Herzfeld, J., Raap, J., and Lugtenburg, J. (2000) *Proc. Natl. Acad. Sci. U.S.A. 97*, 4643−4648.
49. Kandori, H., Kinoshita, N., Yamazaki, Y., Maeda, A., Shichida, Y., Needleman, R., Lanyi, J. K., Bizounok, M., Herzfeld, J., Raap, J., and Lugtenburg, J. (1999) *Biochemistry 38*, 9676−9683.
50. Shimono, K., Furutani, Y., Kamo, N., and Kandori, H. (2003) *Biochemistry 42*, 7801−7806.
51. Bergo, V., Spudich, E. N., Spudich, J. L., and Rothschild, K. J. (2003) *J. Biol. Chem. 278*, 36556−36562.

BI035678G